Body Drawings

Table of Contents

Executive Summary

Adolescent Pediatric Pain Tool (APPT) forms are used to collect data on adolescents' pain before and after major surgery, including diagrams to indicate the location and size (surface area) of the pain on the patient's body. These diagrams, which are filled out on paper, lack clinical utility – they are not easily analyzed over time or incorporated into electronic medical records (EMRs). To solve this problem, open source computer vision library OpenCV was used to digitize body diagrams and extract pain location and surface area. Images were cleaned through a series of morphological transformations to remove noise created by scanners. After cleaning, images were compared to a reference diagram which demarcated each region on the body to determine the degree of pain overlap. With good efficacy (correct classification rate 96.8%, sensitivity 88.0%, and specificity 97.1%) and efficiency (runtime ~2 seconds per image), the model was able to identify the demarcated pain locations. However, additional work is needed to make the model more robust to scanner noise and poorly demarcated pain locations, increase analytical capabilities for clinicians, and integrate easily with electronic medical records.

Introduction

The Adolescent Pediatric Pain Tool (APPT) form contains a body outline diagram (BOD) to facilitate self-reporting of pain sites and associated surface area for adolescents undergoing surgery. Inter-rater reliability for manually coded BOD drawings is only fair to moderate. Drawings are also prone to manual measurement error – subjectivity of the human measurer and difficulty measuring the area enclosed by irregular shapes. The clinical utility, trending capabilities, and interpretability of BOD drawings are significant limitations of the APPT form. A more rigorous method to code BODs and extract data for further analysis is needed. To resolve these limitations, a computer vision approach was explored so that paper diagrams, which are readily available and familiar to clinicians, may be more fully analyzed and easily integrated into digital workflows.

Image Digitization Methods

Data was provided by xxxx and includes scanned APPT forms as well as demographic and medical data for 66 patients undergoing major chest or

spinal surgery. Patients were adolescents with scoliosis or pectus excavatum and data was collected preoperatively, daily postoperatively during hospitalization, and at postoperative visits. At each stage, pain sites and areas were drawn by adolescents on paper BODs, as part of the APPT form, and then scanned, collated, and manually compared to a labeled APPT form (Figure 1). Demographic and medical data included: patient age, gender, surgery type, and pain scores (CPASS, PANAS, YAPFAQ, FDI) at each visit and for up to 14 months following the initial surgery, and was provided in spreadsheet format.

The scanned BOD images were first cleaned with the goal of improving the alignment process. The cleaning process involved removing noise through grayscaling, morphology transformations, thresholding and repeated cropping techniques. Cropping from the top of the image and filling in the image from left and right sides with white was repeated until the aligned image reached a chosen similarity score and number of matches with the reference diagram[1] (Figure 2). The images were aligned with the reference diagram using corner detectors and a homography matrix to identify and match significant points on the BOD. After alignment, the image and reference diagram were blended and their differences identified. The resulting differenced image was cleaned again, this time with the goal of removing all parts of the image that weren't the patient-drawn marks. Finally, the identified marked pixels and corresponding body parts and areas were exported for further analysis (see Table 1 for a sample of the output data).

Image Digitization Results

The model was effective in extracting BOD drawings and identifying pain sites that corresponded to the APPT scoring template. After manually labeling client-provided data and comparing to the model's predictions, the accuracy was calculated at 96.0%, sensitivity at 91.0%, and specificity at 96.2% (see Table 2 in the Appendix for more complete model results). Of course, this manual labeling is subject to human error and is subjective with respect to irregular shapes. It is also worth noting that due to the high number of body areas with no pain, the overall accuracy is highly affected by changes in specificity.

[1] The chosen similarity score was 0.9, while the number of matches was 3,700. These values were chosen after repeated testing.

The model was fairly effective in predicting BSAs. The number of pixels comprising the patient-drawn marks were summed and compared to the actual BSA numbers. However, since pixels and body surface area are not directly comparable, we had to resort to using different statistical methods. The actual BSA numbers were regressed against the predicted pixels so that the pixels may be "scaled" linearly to produce predicted BSA numbers. Our model showed that the variation in raw pixels was able to account for 50.7% of actual BSA variability. Finally, we were able to scale the pixels and actual BSA values by dividing them by the total number of body pixels and the total body outline BSA. The regression and correlation coefficients of the actual and predicted value ratios were almost completely the same as the model produced using raw values (Figures 3 and 4).

Figure 5 shows successful identification of pain locations and markings. Although generally performing well at identifying significant pain locations, the model struggled when locations were not clearly delineated and shaded in – when they were very lightly shaded (as with a pencil or crayon) or not shaded in at all (Figure 6). Lightly-shaded areas are too faint; they are deemed as noise during the cleaning process and accordingly (and incorrectly) removed. Remaining noise is likely what prevents the scanned image from properly aligning with the reference diagram. Because of the misalignment, the edge of the diagram is still visible in the final markings. The process does detect some of the markings on the back, but they are not deemed significant so their corresponding locations are not highlighted. These images are also likely the reason why the ratio sMAPE (symmetric mean absolute percentage error) for images with actual pain was a relatively high 44.3%. This weakness is easily addressed by instructing patients to shade in painful areas and use a pen or dark marker. Additionally, the model was optimized only for those images in the provided dataset – its generalizability to other scanned images, procedures, and pain locations is unknown.

Pain Visualization

Using the detected markings, we produced visuals for patient-specific pain, and surgery-specific pain which overlays marks across all patients for each surgery type. These visuals present clear information on pain location

and development for clinicians and researchers, and they have the added benefit of being safe to share, as all patient identifiers are completely removed.

The external folder contains examples of animated plots showing patient-level and surgery-level pain markings that were documented across all stages of surgery: pre-operation, post-operation, and PD clinics, which occur in the weeks and months after surgery. These animations are particularly useful if a clinician seeks to learn about expected pain locations, identify unexpected pain locations, or determine how many clinic visits a patient should expect post-surgery. Static heatmaps were also created to pain markings aggregated across time (Figure 7, 8, 9). These heatmaps are particularly useful if a clinician needs to see all pain areas for a particular patient or surgery.

Patient Data Analysis

We then transitioned to incorporate the tabular data, which includes patient demographic data as well as opioid usage and pain scores before and after surgery. To analyze the relationship between pain metrics and body location, we merged this dataset of patient pain scores together with our reference of all patient pain locations output during the image digitization process (Figure 10). Because pain scores are not associated with any particular location, and rather logged as an overall body-wide score at that stage, we adjusted pain scores so that any nonzero value is kept only if the digitization model identified at least one pixel of pain in that contour. In other words, a pain score was zeroed out if no pain marking was identified within that body location.

Visualizations were effective in conveying the distribution of pain and covariation between locations. Figure 11 illustrates the wide variation in CPASS scores for each body location. A core group of pain locations is present for each surgery type – not surprisingly, it primarily spans the torso for pectus patients and the back for spine patients. This covariation is made more obvious by Figure 12, which identifies, for a given pain location, which other locations have pain at the same time. We again see primary clusters at the torso and back with some spill-over to the opposite side of the body (anterior vs. posterior). There is little correlation with other parts of the body.

In order to determine whether associations between body areas and pain / function measures are significant, we conducted bi-variate and multivariate statistical analyses. Since pain indicators were recorded per image, we conducted individual independent T-tests and Mann-Whitney U Tests between individual body parts and pain indicators. As shown in Table 4, patients who experienced pain in chest and abdomen areas (both front and back) had significantly higher PANAS, YAPFAQ and CPASS scores. We then proceeded to verify whether these associations continue to be significant when controlling for demographic variables. To model the 66 patients and their images, which are in sense repeated pain measures, we conducted various multivariate ordinal regressions fitted using Generalized Estimating Equations (GEE). The results of the models are shown in Table 5. Our results show that PANAS-positive is negatively associated with pain in area 27 (-43.8%), but has a significant positive association with pain in area 31 (302%). PANAS-negative is significantly associated with pain in area 15 (1568%). Total YAPFAQ score has a positive association with pain in both area 1 (526%) and area 28 (74%). Finally, pain in area 7 is negatively associated with total CPASS (-71.2%) and FDI (-97.3%) scores. These results indicate that patients with pain in the upper back and front pelvis areas experience more pain, while patients with pain in the chest have decreased functional scores.

Conclusion

This computer vision method of processing BODs is accessible, convenient, and provides better sensitivity and specificity for pain site and surface area than manual coding. Extracted data can be further analyzed for trends and modeled for pain trajectory prediction. While the use of digital applications to prospectively collect BOD data may overcome current APPT limitations, loss of historic data, expense, data access, and electronic medical record (EMR) integration present new limitations. Paper BODs are convenient, inexpensive, easily scanned into EMRs, and now easily analyzed through computer vision methods. Although more work needs to be done to improve model sensitivity and robustness, these results indicate a promising avenue for integrating computer vision into clinicians' daily workflow.

References

Fernandes AM, De Campos C, Batalha L, Perdigão A, Jacob E. Pain assessment using the adolescent pediatric pain tool: a systematic review. Pain Res Manag. 2014 Jul-Aug;19(4):212-8. doi: 10.1155/2014/979416.

Fuss S, Pagé G, Katz J. Persistent pain in a community-based sample of children and adolescents. *Pain Res Manag*. 2011;16(5):303-309. doi:10.1155/2011/534652

Jacob E, Mack AK, Savedra M, Van Cleve L, Wilkie DJ. Adolescent pediatric pain tool for multidimensional measurement of pain in children and adolescents. Pain Manag Nurs. 2014 Sep;15(3):694-706. doi: 10.1016/j.pmn.2013.03.002.

Pagé MG, Campbell F, Isaac L, Stinson J, Martin-Pichora AL, Katz J. Reliability and validity of the Child Pain Anxiety Symptoms Scale (CPASS) in a clinical sample of children and adolescents with acute postsurgical pain. Pain. 2011 Sep;152(9):1958-65. doi: 10.1016/j.pain.2011.02.053.

Pagé MG, Fuss S, Martin AL, Escobar EM, Katz J. Development and preliminary validation of the Child Pain Anxiety Symptoms Scale in a community sample. J Pediatr Psychol. 2010 Nov;35(10):1071-82. doi: 10.1093/jpepsy/jsq034.

Appendix

Table 1. Sample output data

Patient	Stage	Predicted locations	Predicted BSA
502	1	6, 7	310.0
502	2	5, 6, 16	178.0
502	3		0.0
502	4	27, 28	248.0

Table 2. Metrics for final model performance

Metric	Performance
Sensitivity (recall)	91.0%
Specificity	96.2%
Accuracy (ACC)	96.0%
AUC	0.945
Runtime	~2s per image (18 min. total)
BSA R-squared / Adj. R-squared	0.507^{***} / 0.506^{***}
BSA Spearman rho	0.788^{***}
sMAPE[1]	0.443

Note: $p < 0.05$: *, $p < 0.01$: **, $p < 0.001$: ***

[1]Symmetric mean absolute percentage error (sMAPE): Calculated using ratios and only with data from body areas with actual pain. The error is calculated for each image (with all pain areas summed).

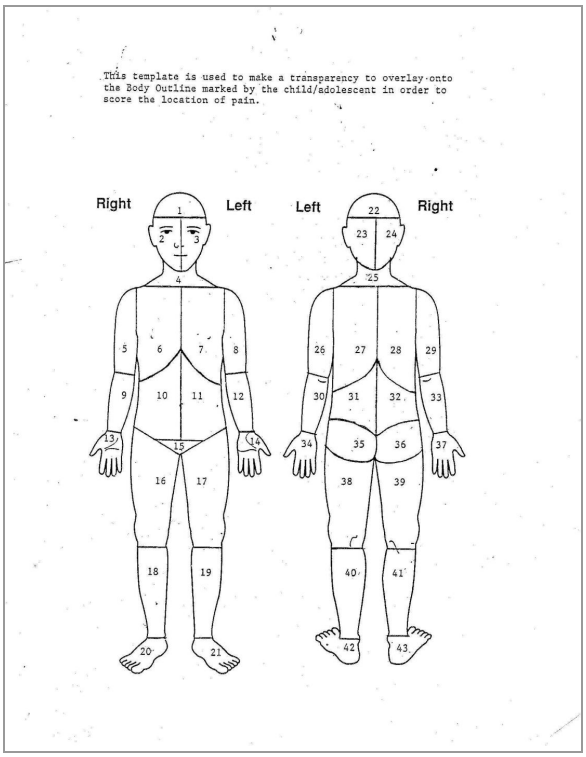

Figure 1. APPT body locations

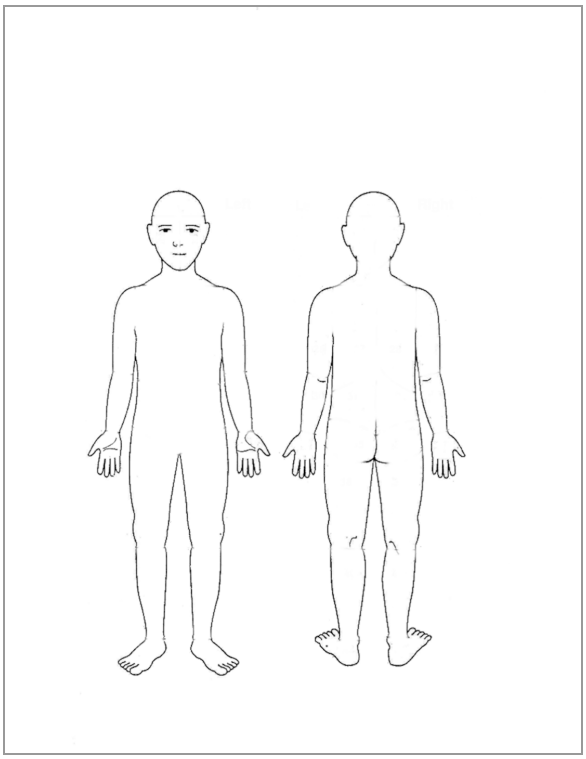

Figure 2. Reference diagram

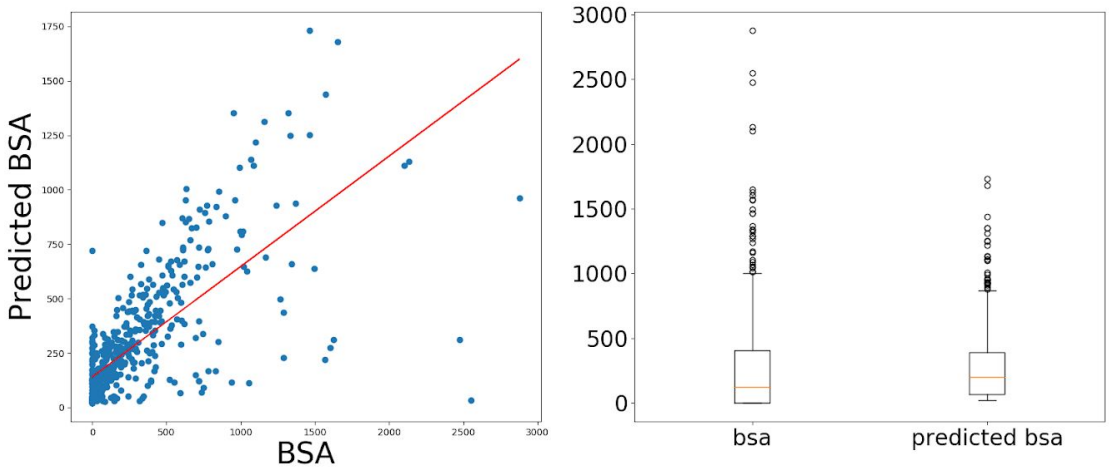

Figure 3. BSA results (raw pixels vs BSA)

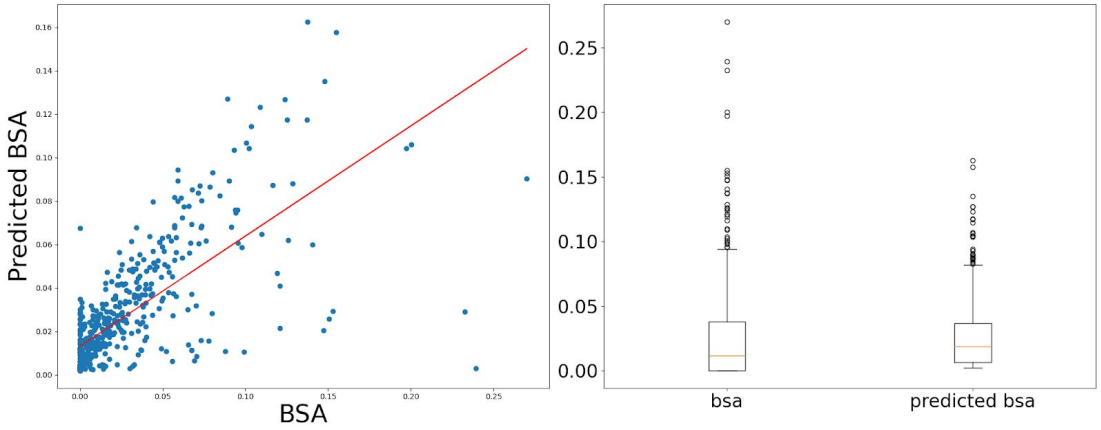

Figure 4. BSA results (ratio to total body pixel/area)

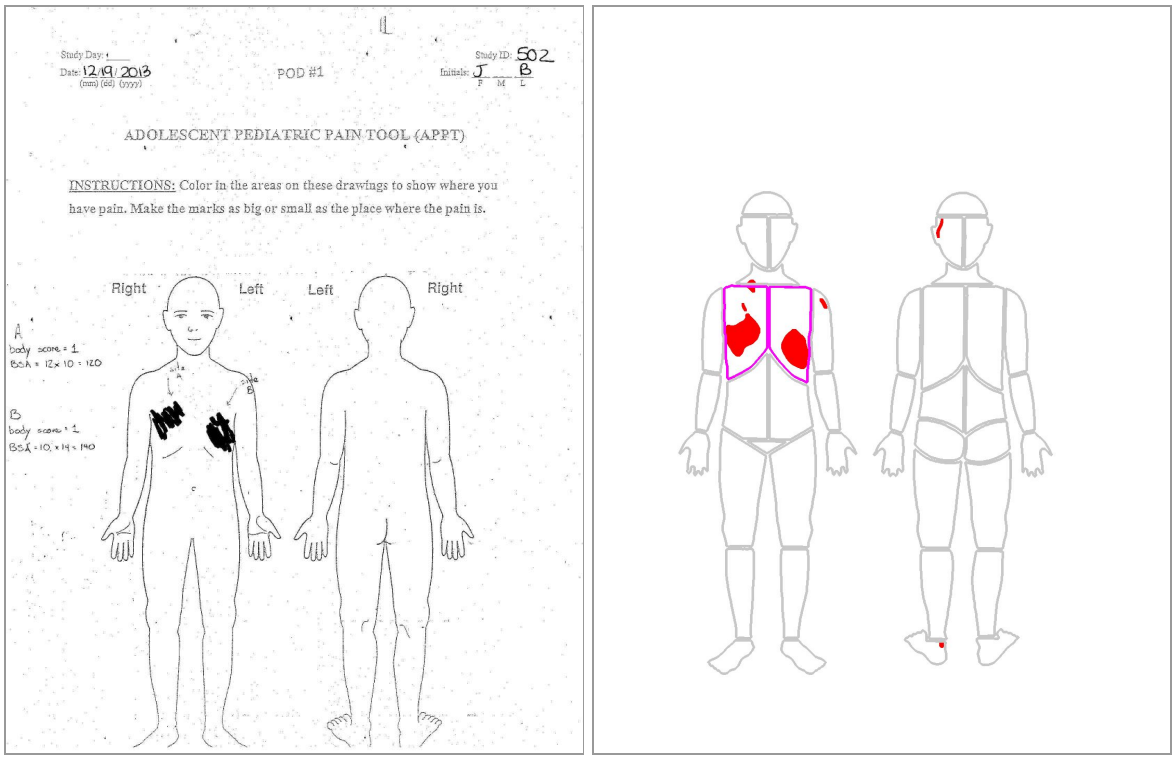

Figure 5. Successful identification of pain locations

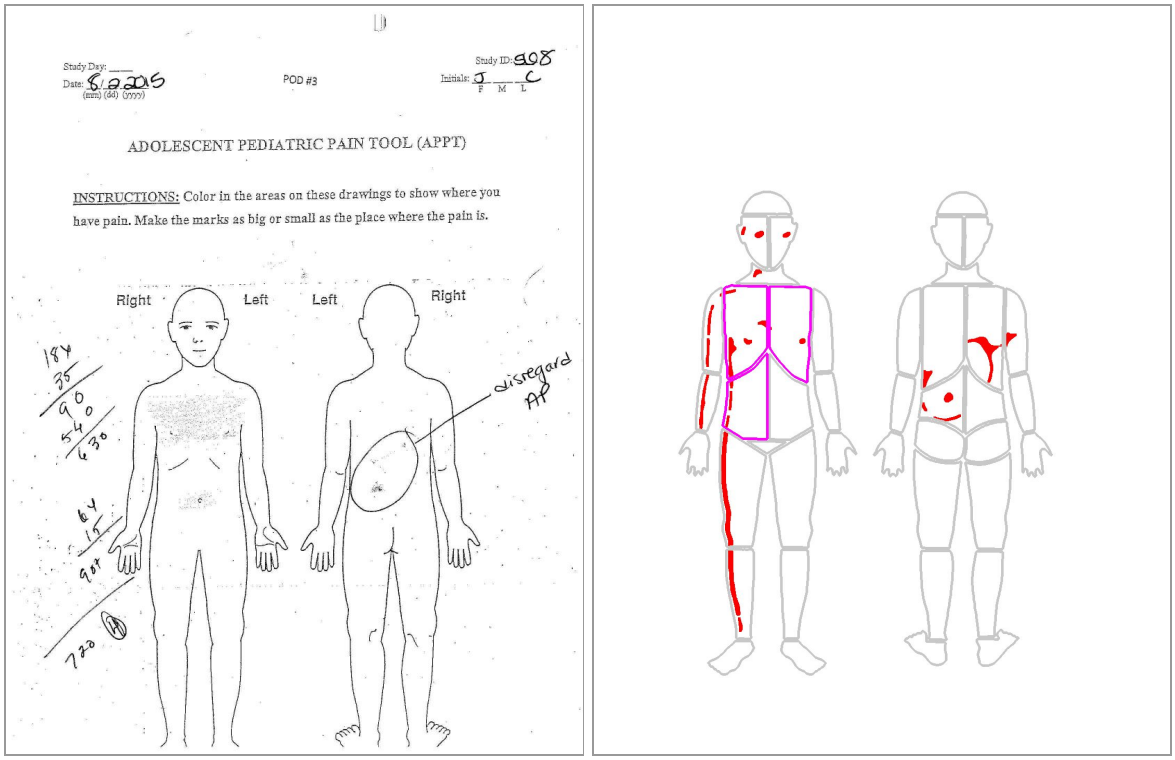

Figure 6. Unsuccessful identification of pain locations

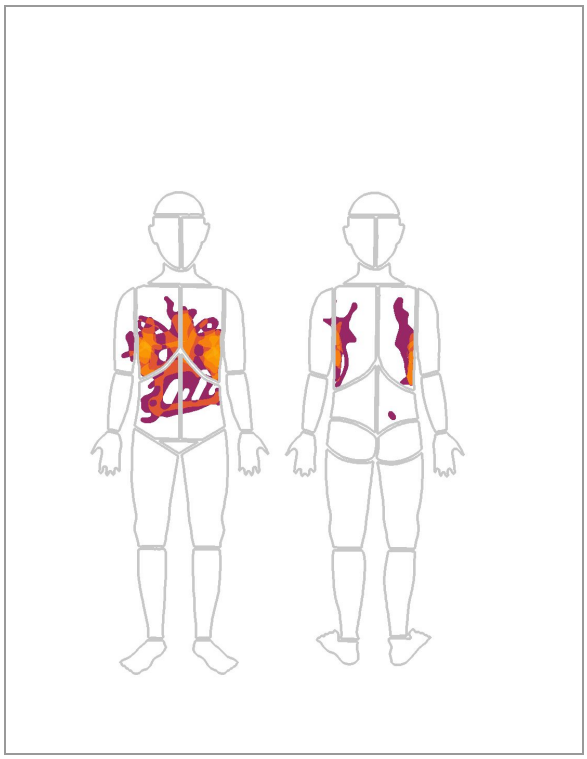

Figure 7. A pectus patient heatmap

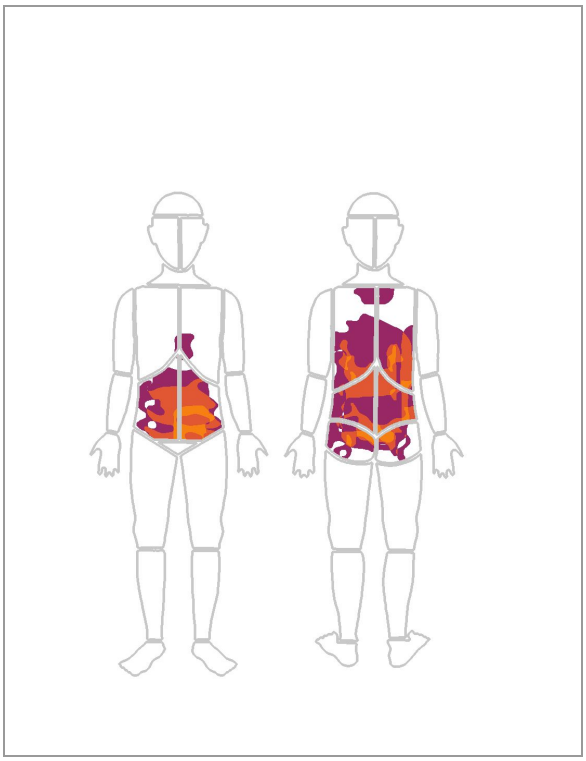

Figure 8. A spine patient heatmap

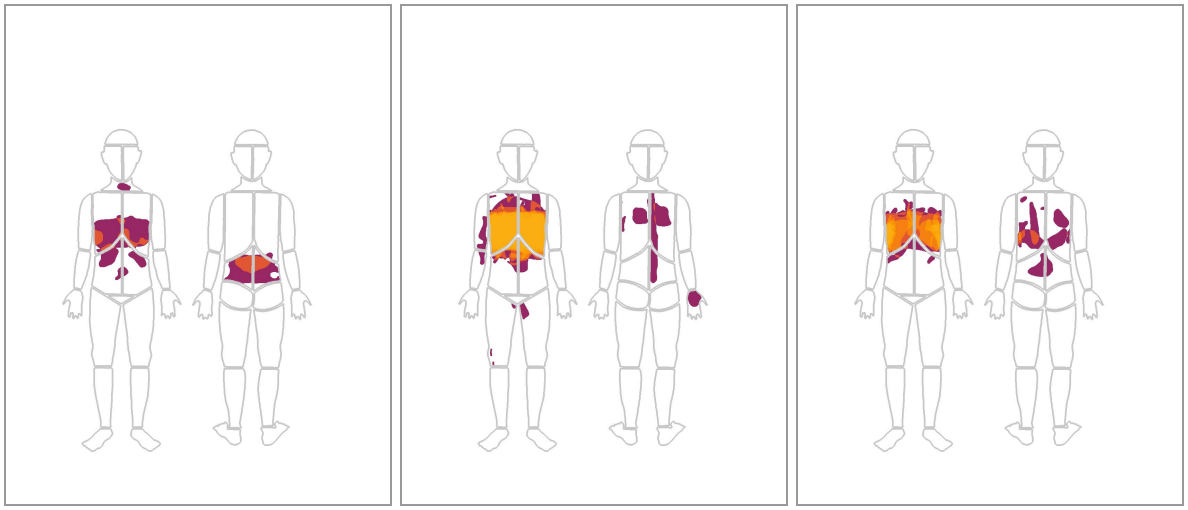

Figure 9. Heatmaps for all pectus surgery patients
Pre-op (L), Post-Operative Day 1 (M), and PD Clinic 1 (R)

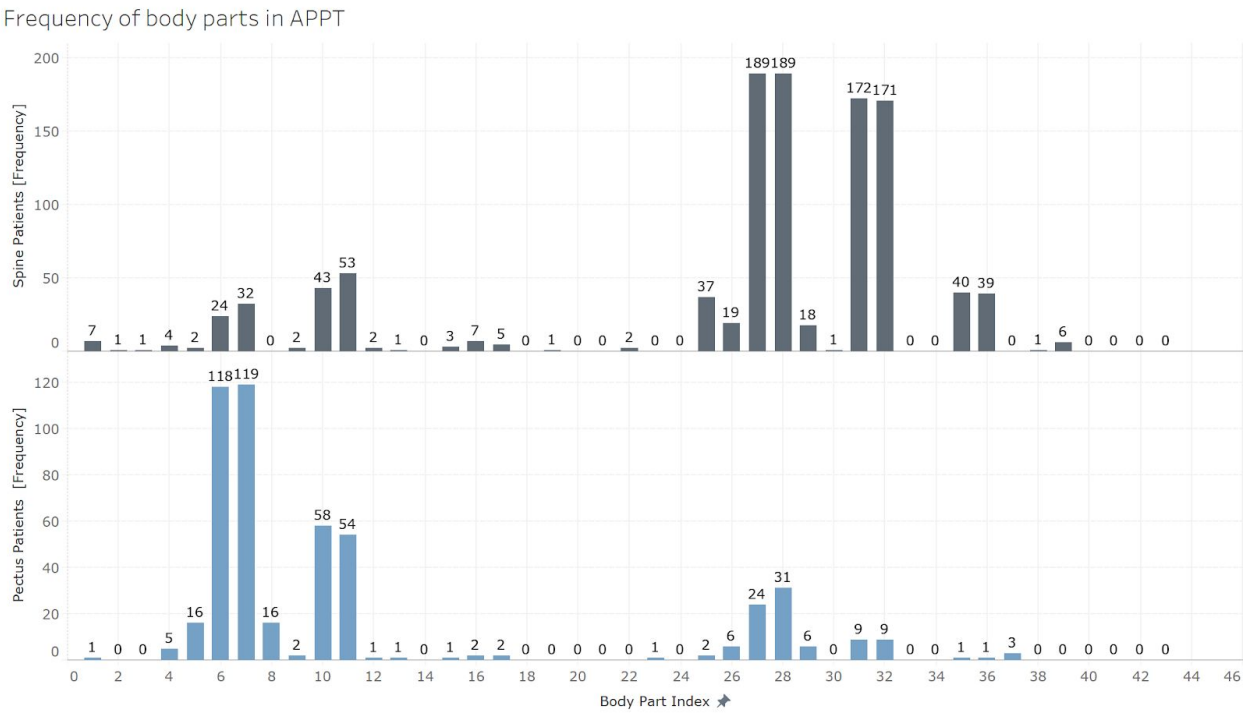

Figure 10. Frequency of pain per location

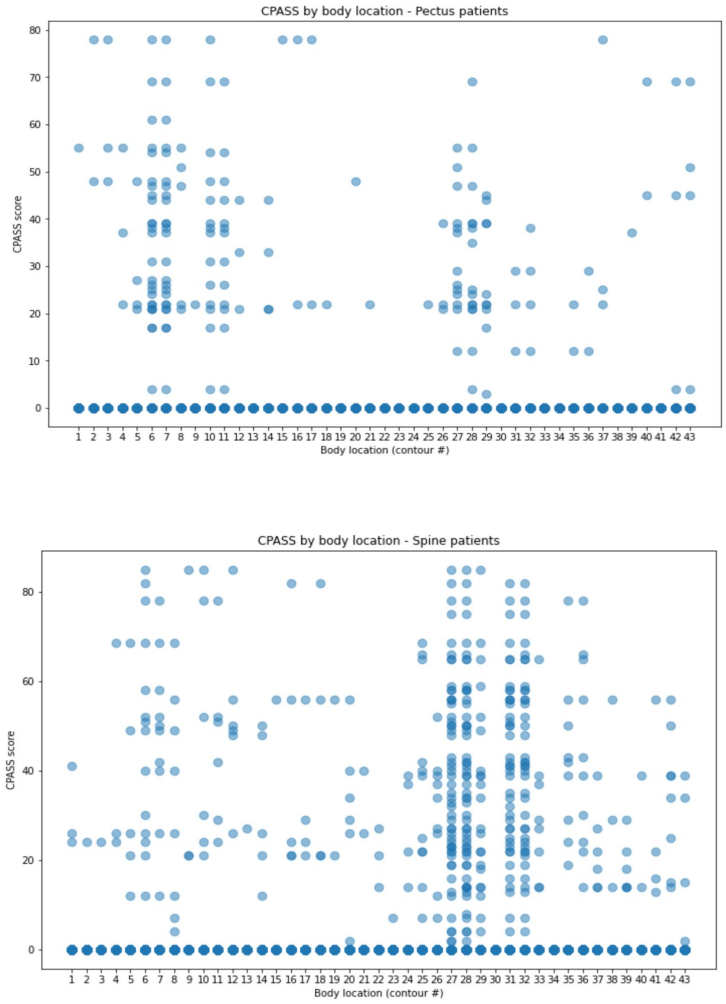

Figure 11. CPASS scores for each location (top: pectus patients, bottom: spine patients)

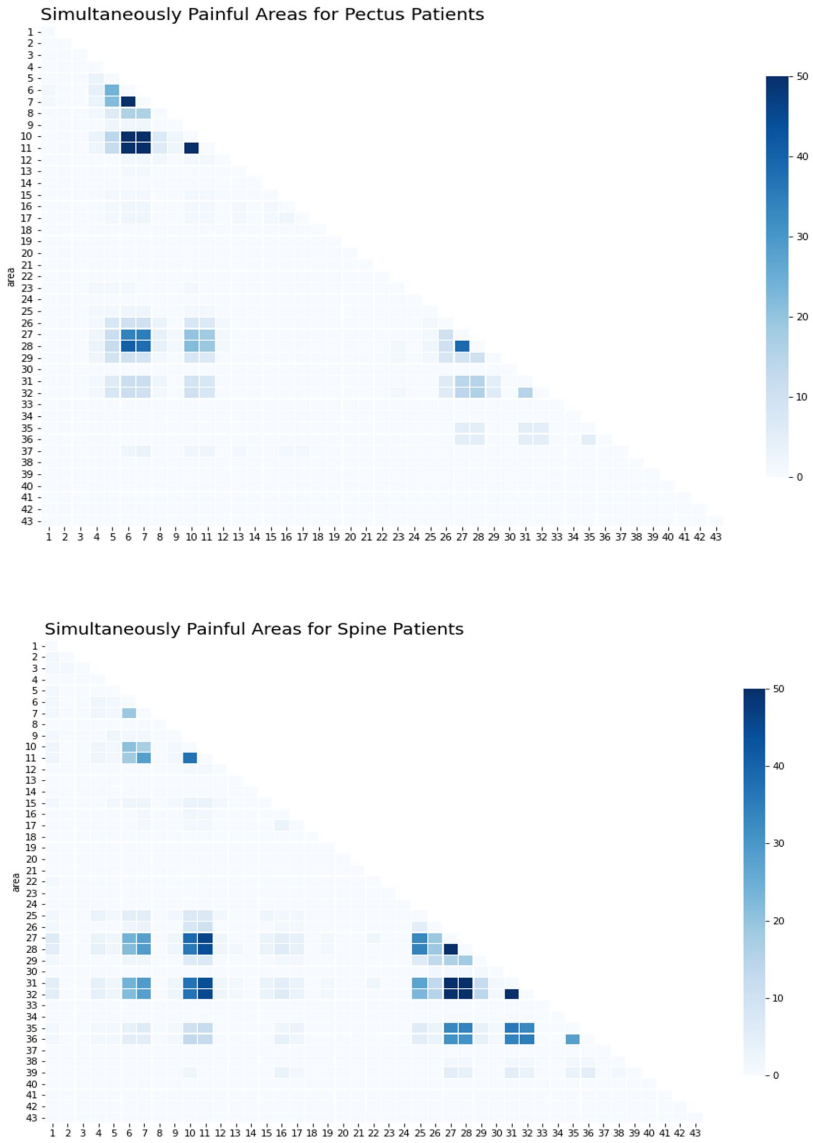

Figure 12. Covariation of pain locations (top: pectus patients, bottom: spine patients)

Table 3. Spearman's rank correlation coefficient for pain scores vs. body location

Pain metric	Pectus patient correlation	Spine patient correlation	P-value (pectus / spine)
CPASS	-0.06	0.05	1.62e-8 / 2.33e-9
PANAS+	-0.12	0.07	8.66e-27 / 3.04e-16
PANAS-	-0.12	0.07	6.17e-27 / 4.47e-15
FDI	0.00	0.02	0.98 / 0.01
YAPFAQ	0.13	0.06	4.01e-29 / 2.68e-12

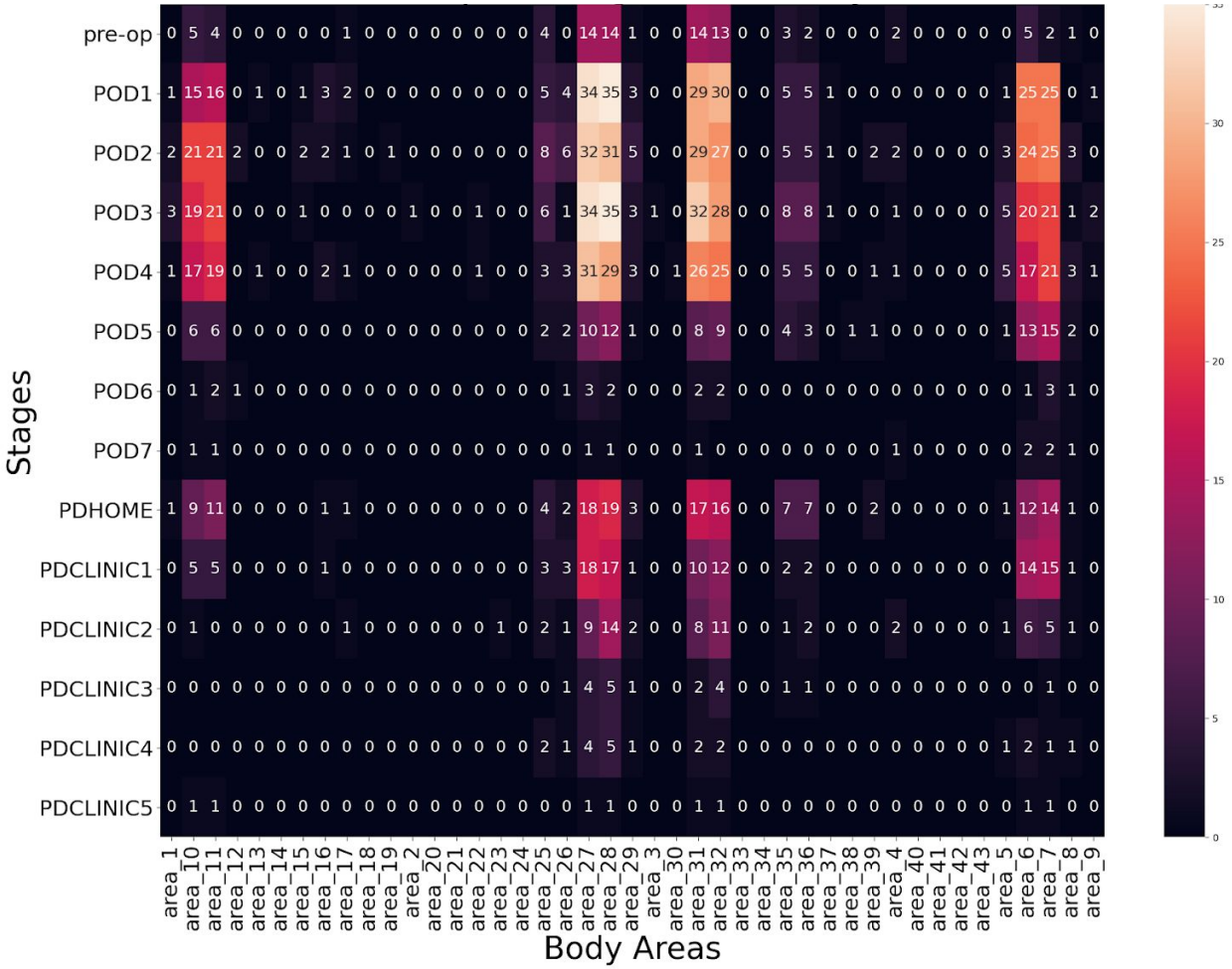

Figure 13. Body area and stage heatmap

Table 4. Associations between body areas and pain / function measures

Body Areas / Normality	PANAS_PositiveT[1]	PANAS_NegativeT[1]	YAPFAQ_Total[1]	CPASS_Total[2]	FDITOTAL[2]
Kurtosis	2.279	2.373	1.842	6.900	39.275
Skewness	0.340	0.142	0.597	2.173	5.738
Area 1	-0.866	-1.852	-3.114**	2173.000	2144.000
Area 2	0.037	-0.770	-1.875	308.500	271.500
Area 3	0.037	-0.770	-1.875	308.500	271.500
Area 4	-1.433	-0.726	0.083	2179.000	2154.500
Area 5	-1.011	-1.121	-2.851**	5400.000*	4734.000
Area 6	0.073	-1.468	-5.303***	27076.000	27385.500**
Area 7	0.542	-0.513	-5.435***	29034.000***	29309.000***
Area 8	0.914	-0.078	-1.519	4622.000	4224.000
Area 9	-1.331	-1.458	-1.987*	1228.000	1080.000
Area 10	-2.269*	-4.441***	-5.258***	21488.000	21444.000*
Area 11	-1.833	-3.658***	-5.115***	22414.000	22973.000**
Area 12	-0.974	-3.682***	-1.427	922.500	811.500
Area 13	-1.831	-0.152	-1.422	309.000	542.000
Area 15	-1.042	-4.089***	-13.587***	919.500	1080.000
Area 16	-0.202	-0.666	-1.375	2140.000	2407.500
Area 17	-0.284	-0.975	-1.305	1293.000	1635.000
Area 19	0.037	-1.212	0.891	308.500	271.500
Area 22	-0.811	-1.782	-1.285	616.000	542.000
Area 23	-0.178	-0.063	0.313	308.500	271.500
Area 25	0.067	-2.276*	-1.748**	9317.000	9594.500
Area 26	0.071	-1.294	-2.437*	6375.000	6487.500
Area 27	-1.389	-4.641***	-5.699***	30627.500	31837.000
Area 28	-1.841	-4.783***	-5.879***	30089.000	31998.500
Area 29	0.424	-1.167	-2.415*	6125.500	6240.000
Area 30	1.185	1.262	0.891	308.500	271.500
Area 31	-3.702***	-5.742***	-5.565***	26959.000	29610.000

Area 32	-2.590*	-5.265***	-4.976***	26827.000	28989.000
Area 35	-1.168	-1.968	-1.080	9441.500	9272.500
Area 36	-0.584	-1.833	-0.996	9649.000	9305.000
Area 37	-1.515	-1.732	-1.689	615.500	811.500
Area 38	-1.399	-0.858	-1.229	308.500	271.500
Area 39	-1.057	0.279	-0.731	1836.000	1614.000

Note: $p < 0.05$: *, $p < 0.01$: **, $p < 0.001$: ***. Only body areas with pain are included in this table.

[1]Associations between body areas and normally distributed continuous variables were calculated using independent T-tests (Levene's Test was first performed to determine whether variances are unequal).

[2]Associations between body areas and non-normally distributed continuous variables were calculated using Mann-Whitney U Tests.

Table 5. Multivariate associations between body areas and pain / function measures

Variables	PANAS_PositiveT	PANAS_NegativeT	YAPFAQ_Total	CPASS_Total	FDITOTAL
Demographics					
Gender	Ref. Male				
Female	1.148	1.422	1.004	1.312	2.921*
Surgery type	Ref. Nuss				
Spine	0.875	0.887	0.931	0.660	0.467
Age	1.014*	1.005	1.004	1.002	1.007
Weight	0.989	0.992	0.999	0.991	0.997
Body Areas					
Area 1			5.259***		
Area 7				0.287*	0.027**
Area 15		15.680**			
Area 27	0.562*				
Area 28			1.736*		
Area 31	3.025***				

Note 1: Coefficients shown in the table are adjusted odds ratios. $p < 0.05$: *, $p < 0.01$: **, $p < 0.001$: ***.

Note 2: Due to the high number of body areas included in each model, only areas with significance in at least one of the models are shown.

Variables used in each model (areas with no greater than 0 value of the regressed measure were excluded)

1. PANAS_PositiveT:
    - gender, surgery, age, weight, area 1, area 5, area 6, area 7, area 9, area 10, area 11, area 12 area 15, area 25, area 26, area 27, area 28, area 29, area 31, area 32
2. PANAS_NegativeT
    - gender, surgery, age, weight, area 1, area 5, area 6, area 7, area 9, area 10, area 11, area 12 area 15, area 25, area 26, area 27, area 28, area 29, area 31, area 32
3. YAPFAQ_Total
    - gender, surgery, age, weight, area 1, area 5, area 6, area 7, area 9, area 10, area 11, area 12 area 15, area 25, area 26, area 27, area 28, area 29, area 31, area 32
4. CPASS_Total
    - gender, surgery, age, weight, area 1, area 6, area 7, area 10, area 11, area 15, area 25, area 26, area 27, area 28, area 29, area 31, area 32
5. FDITOTAL
    - gender, surgery, age, weight, area 6, area 7, area 10, area 11, area 25, area 27, area 28, area 31, area 32